Handbook of Green Chemistry

Edited by Paul T. Anastas

WILEY-VCH

Green Catalysis

Volume 2: Heterogeneous Catalysis

Volume Editor:
Robert H. Crabtree

Handbook of Green Chemistry

Volume 2
Heterogenous Catalysis

Volume Edited by
Robert H. Crabtree

Related Titles

Wasserscheid, P., Welton, T. (eds.)

Ionic Liquids in Synthesis

2nd Edition
2008
ISBN: 978-3-527-31239-9

Sheldon, R. A., Arends, I., Hanefeld, U.

Green Chemistry and Catalysis

2007
ISBN: 978-3-527-30715-9

Cornils, B., Herrmann, W. A., Muhler, M., Wong, C. - H. (eds.)

Catalysis from A - Z

A Concise Encyclopedia

3rd Edition
2007
ISBN: 978-3-527-31438-6

Loupy, A. (ed.)

Microwaves in Organic Synthesis

2nd Edition
2006
ISBN: 978-3-527-31452-2

Kappe, C. O., Stadler, A., Mannhold, R., Kubinyi, H., Folkers, G. (eds.)

Microwaves in Organic and Medicinal Chemistry

2005
ISBN: 978-3-527-31210-8

Edited by
Paul T. Anastas

Handbook of Green Chemistry – Green Catalysis

Volume 2
Heterogenous Catalysis

Volume Edited by Robert H. Crabtree

WILEY-VCH Verlag GmbH & Co. KGaA

Series Editor

Prof. Dr. Paul T. Anastas
Yale University
Center for Green Chemistry & Green Engineering
225 Prospect Street
New Haven, CT 06520
USA

Volume Editor

Prof. Dr. Robert H. Crabtree
Yale University
Department of Chemistry
225 Prospect St.
New Haven, CT 06520
USA

Graphiker: Adam

Handbook of Green Chemistry
ISBN (12 volumes): 978-3-527-31404-1

Set 1 Green Catalysis 978-3-527-31577-2
Volume 1: Homogeneous Catalysis
Set 2 Green Solvents 978-3-527-31574-1
Volume 2: Heterogeneous Catalysis
Set 3 Green Processes 978-3-527-31576-5
Volume 3: Biocatalysis
Set 4 Green Products 978-3-527-31575-8

The cover picture contains images from Corbis Digital Stock (Dictionary) and PhotoDisc, Inc./Getty Images (Flak containing a blue liquid).

Library of Congress Card No.:
applied for

British Library Cataloguing-in-Publication Data
A catalogue record for this book is available from the British Library.

Bibliographic information published by the Deutsche Nationalbibliothek
The Deutsche Nationalbibliothek lists this publication in the Deutsche Nationalbibliografie; detailed bibliographic data are available on the Internet at http://dnb.d-nb.de.

Typesetting Thomson Digital, Noida, India
Printing betz-druck GmbH, Darmstadt
Binding Litges & Dopf GmbH, Heppenheim
Cover Design Adam-Design, Weinheim

Printed in the Federal Republic of Germany
Printed on acid-free paper

ISBN: 978-3-527-32497-2

Contents

About the Editors *XIII*
List of Contributors *XV*

1 Zeolites in Catalysis *1*
Stephen H. Brown
1.1 Introduction *1*
1.1.1 The Environmental Benefits of Zeolite-enabled Processes *2*
1.2 General Process Considerations *5*
1.3 Zeolite Fundamentals *6*
1.3.1 Other Properties *7*
1.3.2 Number of Acid Sites *8*
1.3.3 Acid Strength *8*
1.4 Reaction Mechanisms *8*
1.4.1 Hydrocarbon Cracking *8*
1.4.2 Oligomerization and Alkylation *12*
1.4.3 Isomerization *14*
1.4.4 Transalkylation of Aromatics *15*
1.4.5 Hydrogen Transfer or Conjunct Polymerization *18*
1.5 Mass Transport and Diffusion *21*
1.6 Zeolite Shape Selectivity *22*
1.6.1 Mass Transport Discrimination of Product Molecules *22*
1.6.2 Molecular Sieving *23*
1.6.3 Molecular Orientation *23*
1.6.4 Transition State Stabilization *25*
1.6.5 Organic Reaction Centers *26*
1.7 Counter Ion Mobility *29*
1.8 Conclusions *29*
References *29*

2 Sol–Gel Sulfonic Acid Silicas as Catalysts *37*
Adam F. Lee and Karen Wilson
2.1 Introduction *37*
2.2 Preparation of Meso–structured Silica Sulfonic Acid Catalysts *38*

Handbook of Green Chemistry, Volume 2: Heterogeneous Catalysis. Edited by Robert H. Crabtree

ISBN: 978-3-527-32497-2

2.2.1 Templating Methods *38*
2.2.1.1 Cationic/Anionic Templates *38*
2.2.1.2 Neutral Templates *39*
2.2.2 Organically Functionalized Silica *39*
2.2.2.1 Characterization *40*
2.2.2.2 Grafting Methods *42*
2.2.2.3 Direct Preparation Methods *43*
2.2.3 Acid Strength of Sulfonic Acid Catalysts *44*
2.2.3.1 Phenyl- Versus Propylsulfonic Acids *45*
2.2.4 Fine Tuning the Catalytic Activity of Sulfonic Acid Silicas *46*
2.2.4.1 Cooperative Effects *46*
2.2.4.2 Effect of Spectator Groups *48*
2.3 Application in Organic Transformations *49*
2.3.1 Condensation and Esterification *49*
2.3.2 Electrophilic Aromatic Substitution *51*
2.3.3 Miscellaneous Reactions *52*
2.4 Conclusions and Future Prospects *53*
References *55*

3 Applications of Environmentally Friendly TiO_2 Photocatalysts in Green Chemistry: Environmental Purification and Clean Energy Production Under Solar Light Irradiation *59*
Masaya Matsuoka and Masakazu Anpo
3.1 Introduction *59*
3.2 Principles of Photocatalysis *61*
3.3 Application of Photocatalysts in Green Chemistry: Solar Energy Conversion and Environmental Protection *62*
3.3.1 Water Splitting to Produce Pure Hydrogen as Clean Fuel *62*
3.3.2 Photocatalytic Reduction of CO_2 with H_2O (Artificial Photosynthesis) *64*
3.3.3 Direct Photocatalytic Decomposition of NO into N_2 and O_2 *67*
3.3.4 Application to the Purification of Air Polluted with Various Organic Compounds *70*
3.3.5 Application to the Purification of Water Polluted with Toxic Compounds Such as Dioxins *71*
3.3.6 Superhydrophilic Properties of TiO_2 Thin Films and Their Application in Self-cleaning Materials *72*
3.4 Development of Visible Light-responsive TiO_2 Photocatalysts *73*
3.4.1 Modification of the Electronic State of TiO_2 by Applying an Advanced Metal Ion Implantation Method *73*
3.4.2 Design of Visible Light-responsive Ti/Zeolite Catalysts by Applying an Advanced Metal Ion Implantation Method *75*
3.4.3 Preparation of Visible Light-responsive TiO_2 Thin-film Photocatalysts by an RF Magnetron Sputtering Deposition Method *76*

3.5 Conclusion *79*
References *79*

4 Nanoparticles in Green Catalysis *81*
Mazaahir Kidwai
4.1 Introduction *81*
4.2 Advanced Catalysis by Gold Nanoparticles *81*
4.3 Nickel Nanoparticles: a Versatile Green Catalyst *85*
4.4 Copper Nanoparticles: an Efficient Catalyst *87*
4.5 Bimetallic Nanoparticles in a Variety of Reactions *89*
References *91*

5 'Heterogreeneous Chemistry' *93*
Heiko Jacobsen
5.1 Introduction *93*
5.2 'Heterogreeneous Catalysis' *96*
5.2.1 An Exemplarily Reaction – Catalysts for Hydrogen Production from Biomass-Derived Hydrocarbons *97*
5.2.2 Transportation Fuels from Biomass – Catalytic Processing of Biomass-derived Reactants *100*
5.2.3 Diesel Fuels from Biomass – Heterogreeneous Processes for Biodiesel Production *103*
5.2.4 Other Heterogreeneous Aspects of Catalysis *106*
5.2.4.1 Solid and Solid Acid Catalysts *106*
5.2.4.2 Recycling Catalysts *107*
5.2.4.3 One-pot Catalysis *108*
5.2.4.4 Photocatalysis *108*
5.3 Solvents for Green Catalysis *108*
5.3.1 Heterogreeneous Solvent Systems *109*
5.3.2 Solvent-free 'Heterogreeneous Chemistry' *112*
5.4 Conclusion and Outlook *113*
References *114*

6 Single-site Heterogeneous Catalysts via Surface-bound Organometallic and Inorganic Complexes *117*
Christophe Copéret
6.1 Introduction *117*
6.2 Generalities *117*
6.3 Hydrogenation and Hydrosilylation *119*
6.3.1 Hydrogenation *119*
6.3.2 Hydrosilylation *123*
6.4 Metathesis and Homologation Processes of Alkenes *124*
6.4.1 Alkene Metathesis *124*
6.4.1.1 Silica-supported Catalysts *124*
6.4.1.2 Alumina-supported Catalysts *127*

6.4.2 Other Alkene Homologation Processes *128*
6.4.2.1 Direct Conversion of Ethene into Propene *128*
6.4.2.2 Cyclization of Dienes *129*
6.5 Metathesis, Dimerization, Trimerization and Other Reactions Involving Alkynes *129*
6.5.1 Alkyne Metathesis *129*
6.5.2 Dimerization and Trimerization of Alkynes *130*
6.5.3 Hydroamination of Alkynes *131*
6.6 Lewis Acid-catalyzed Reactions *131*
6.6.1 Silica-supported Group 4 Metals *131*
6.6.1.1 Reduction of Ketones Through Hydrogen Transfer *133*
6.6.1.2 Transesterification of Esters *134*
6.6.2 Silica-supported Group 3 Metals and Lanthanides *134*
6.7 Oxidation *135*
6.7.1 Single-site Titanium Species *135*
6.7.2 Single-site Zirconium Species *137*
6.7.3 Single-site Vanadium Species *137*
6.7.4 Single-site Tantalum Species *137*
6.7.5 Single-site Group 6 Species *138*
6.7.6 Single-site Iron Species *139*
6.7.7 Single-site Cobalt Species *141*
6.8 Alkane Homologation *141*
6.8.1 Alkane Hydrogenolysis *141*
6.8.2 Alkane Metathesis *143*
6.8.3 Alkane Cross-metathesis *146*
References *146*

7 Sustainable Heterogeneous Acid Catalysis by Heteropoly Acids *153*
Ivan Kozhevnikov
7.1 Introduction *153*
7.2 Development of HPA Catalysts Possessing High Thermal Stability *156*
7.3 Modification of HPA Catalysts to Enhance Coke Combustion *157*
7.3.1 Propene Oligomerization *158*
7.3.2 Friedel–Crafts Acylation *159*
7.4 Inhibition of Coke Formation on HPA Catalysts *161*
7.5 Reactions in Supercritical Fluids *163*
7.6 Cascade Reactions Using Multifunctional HPA Catalysts *165*
7.6.1 Synthesis of MIBK *166*
7.6.2 Hydrogenolysis of Glycerol to Propanediol *167*
7.6.3 Synthesis of Menthol from Citronellal *170*
7.7 Conclusion *172*
References *172*

8 The Kinetics of TiO_2-based Solar Cells Sensitized by Metal Complexes *175*
Anthony G. Fitch, Don Walker, and Nathan S. Lewis
8.1 Introduction *175*
8.2 History *176*
8.3 DSSC Design *177*
8.4 Function of the DSSC *178*
8.5 Performance of a DSSC *179*
8.6 Kinetics Processes *180*
8.7 Charge Injection *181*
8.8 Recombination to the Dye *184*
8.9 Regeneration *187*
8.10 Conclusion *190*
References *192*

9 Automotive Emission Control: Past, Present and Future *197*
Robert J. Farrauto and Jeffrey Hoke
9.1 Introduction *197*
9.2 The First Oxidation Catalysts (1975–80) *198*
9.2.1 Pollution Abatement Reactions for Gasoline-Fueled Engines *198*
9.2.2 Catalyst Materials *199*
9.2.3 Carriers *201*
9.3 Three-Way Catalysis (1980–present) *202*
9.3.1 Three-Way Catalysis *202*
9.3.2 Oxygen or Lambda Sensor *203*
9.3.3 Oxygen Storage Component *203*
9.3.4 Further Improvements in TWC *204*
9.4 Diesel Catalysis *206*
9.4.1 Controlling Diesel Emissions *206*
9.4.2 Diesel Emissions *207*
9.4.3 Diesel Oxidation Catalysts (DOCs): the Past *208*
9.5 Diesel Emission Control: the Future *210*
9.5.1 Catalytic Solutions for the Existing Diesel IC Engine *210*
9.5.2 The Homogeneous Charge Compression Ignition Engine (HCCI) and Advanced Engine Technology *213*
9.6 Fuel Cells and the Hydrogen Economy for Transportation Applications: the Future *217*
9.6.1 The Fuel Cell *217*
9.6.2 Fuel Cells for Transportation *218*
9.6.3 The Hydrogen Service Station *219*
9.7 Conclusions *220*
References *220*

10 Heterogeneous Catalysis for Hydrogen Production *223*
Morgan S. Scott and Hicham Idriss
10.1 Introduction *223*

10.1.1 Renewable Energy *224*
10.1.2 Hydrogen *225*
10.1.3 Hydrogen from Ethanol Decomposition *226*
10.1.4 Catalytic Oxidation *228*
10.1.5 Steam Reforming *228*
10.1.6 Dry Reforming *229*
10.1.7 Water Gas Shift Reaction (WGSR) *229*
10.1.8 Catalytic Reforming of Methane *230*
10.1.9 Thermodynamics *230*
10.2 Catalysis *231*
10.2.1 The Noble Metals Pd and Rh *232*
10.2.2 Structure and Properties of Cerium Dioxide *233*
10.2.3 Noble Metal/Ceria Catalysts *235*
10.2.4 Adsorption of Ethanol *236*
10.2.5 Adsorption of Water *236*
10.2.6 Adsorption of Carbon Oxides *237*
10.2.7 Hydrides *237*
10.3 Catalytic Decomposition of Ethanol *238*
10.3.1 Ethanol on Metal Oxides *238*
10.3.2 Ethanol on a Noble Metal/Ceria Surface *239*
10.3.3 Catalytic Oxidation of Ethanol *242*
10.3.4 Catalytic Reforming of Ethanol *243*
10.4 Conclusions *244*
References *245*

11 High-Throughput Screening of Catalyst Libraries for Emissions Control *247*
Stephen Cypes, Joel Cizeron, Alfred Hagemeyer, and Anthony Volpe
11.1 Introduction *247*
11.1.1 Introduction to High-Throughput Heterogeneous Catalysis *247*
11.1.2 The Hierarchical Workflow in Heterogeneous Catalysis *248*
11.1.3 Applications to Green Chemistry *249*
11.2 Experimental Techniques and Equipment *250*
11.2.1 Overview of Hardware and Methodologies for Combinatorial Heterogeneous Catalysis *250*
11.2.2 Experimental High-Throughput Workflow for Low-Temperature CO Oxidation and VOC Combustion *259*
11.2.2.1 Primary Synthesis Methods *260*
11.2.2.2 Secondary Synthesis Methods *260*
11.2.2.3 IR Thermography Reactor *261*
11.2.2.4 Multi-Channel Fixed-bed Reactor *263*
11.2.3 Experimental High-Throughput Workflow for NO_x Abatement *263*
11.2.3.1 Primary Synthesis Methods *263*
11.2.3.2 Primary Screening Methods *263*
11.2.3.3 Data Analysis for NO_x Abatement from SMS *264*

11.3 Low-Temperature CO Oxidation and VOC Combustion *265*
11.4 NO_x Abatement *273*
11.5 Conclusion *277*
11.5.1 Application of High-Throughput Screening to Emissions Control *277*
11.5.2 Future Trends in Combinatorial Catalysis *278*
References *278*

12 Catalytic Conversion of High-Moisture Biomass to Synthetic Natural Gas in Supercritical Water *281*
Frédéric Vogel
12.1 Introduction *281*
12.1.1 Heterogeneous Catalysis in Hydrothermal Medium at the Origin of Life? *281*
12.1.2 Biomethane – a Green and Sustainable Fuel *282*
12.1.3 Energetic Potentials *283*
12.1.4 Nutrient Cycles *284*
12.2 Survey of Different Technologies for the Production of Methane from Carbonaceous Feedstocks *285*
12.2.1 Anaerobic Digestion *285*
12.2.2 Thermal Processes *286*
12.3 Water as Solvent and Reactant *288*
12.3.1 Solubility of Organic compounds and Gases *289*
12.3.2 Solubility of Salts *290*
12.4 The Role of Heterogeneous Catalysis *290*
12.4.1 Experimental Methods *290*
12.4.2 Thermodynamic Stability of Methane under Hydrothermal Conditions *291*
12.4.3 Main Reactions of Biomass Gasification *293*
12.4.4 Homogeneous, Non-catalyzed Pathways in Hot Compressed Water *294*
12.4.5 Heterogeneously Catalyzed Pathways in Hot Compressed Water *297*
12.4.6 Active Metals Suited to Hydrothermal Conditions *298*
12.4.6.1 Methanation and Steam Reforming Catalysts *299*
12.4.6.2 Nickel *302*
12.4.6.3 Ruthenium *305*
12.4.7 Catalyst Supports Suited to Hydrothermal Conditions *306*
12.4.8 Deactivation Mechanisms in a Hydrothermal Environment *312*
12.4.8.1 Coke Formation *312*
12.4.8.2 Sintering *314*
12.4.8.3 Poisoning *314*
12.5 Continuous Catalytic Hydrothermal Process for the Production of Methane *315*
12.5.1 Overview of Processes *315*

12.5.2 PSI's Catalytic Hydrothermal Gasification Process *315*
12.5.2.1 Continuous Salt Precipitation and Separation *316*
12.5.2.2 Status *318*
12.6 Summary and Conclusions *318*
12.7 Outlook for Future Developments *319*
12.7.1 A Self-sustaining Biomass Vision (SunCHem) *319*
References *320*

Index *325*

About the Editors

Series Editor

Paul T. Anastas joined Yale University as Professor and serves as the Director of the Center for Green Chemistry and Green Engineering there. From 2004–2006, Paul was the Director of the Green Chemistry Institute in Washington, D.C. Until June 2004 he served as Assistant Director for Environment at the White House Office of Science and Technology Policy where his responsibilities included a wide range of environmental science issues including furthering international public-private cooperation in areas of Science for Sustainability such as Green Chemistry. In 1991, he established the industry-government-university partnership Green Chemistry Program, which was expanded to include basic research, and the Presidential Green Chemistry Challenge Awards. He has published and edited several books in the field of Green Chemistry and developed the 12 Principles of Green Chemistry.

Volume Editor

Robert Crabtree took his first degree at Oxford, did his Ph.D. at Sussex and spent four years in Paris at the CNRS. He has been at Yale since 1977. He has chaired the Inorganic Division at ACS, and won the ACS and RSC organometallic chemistry prizes. He is the author of an organometallic textbook, and is the editor-in-chief of the Encyclopedia of Inorganic Chemistry and Comprehensive Organometallic Chemistry. He has contributed to C-H activation, H_2 complexes, dihydrogen bonding, and his homogeneous tritiation and hydrogenation catalyst is in wide use. More recently, he has combined molecular recognition with CH hydroxylation to obtain high selectivity with a biomimetic strategy.

Handbook of Green Chemistry, Volume 2: Heterogeneous Catalysis. Edited by Robert H. Crabtree

ISBN: 978-3-527-32497-2

List of Contributors

Masakazu Anpo
Osaka Prefecture University
Graduate School of Engineering
Department of Applied Chemistry
Gakuen-chi, 1-1
Sakai
Osaka 599-8531
Japan

Stephen H. Brown
EMRE CSR
1545 Route 22 East
Annandale, NJ 08801
USA

Joel Cizeron
Symyx Technologies, Inc.
3100 Central Expressway
Santa Clara, CA 95051
USA

Christophe Copéret
Université de Lyon
Institut de Chimie de Lyon
Laboratoire C2P2 – ESCPE Lyon
43 boulevard du 11 Novembre 1918
69616 Villeurbanne
France

Stephen Cypes
Symyx Technologies, Inc.
3100 Central Expressway
Santa Clara, CA 95051
USA

Robert J. Farrauto
BASF Catalysts
25 Middlesex–Essex Turnpike
Iselin, NJ 08830
USA

Anthony G. Fitch
California Institute of Technology
Division of Chemistry and Chemical Engineering
Beckman Institute and Kavli Nanoscience Institute
210 Noyes Laboratory, 127–72
Pasadena, CA 91125
USA

Alfred Hagemeyer
Süd-Chemie AG
Waldheimer Strasse 13
83052 Bruckmühl
Germany

Jeffrey Hoke
BASF Catalysts
25 Middlesex–Essex Turnpike
Iselin, NJ 08830
USA

Handbook of Green Chemistry, Volume 2: Heterogeneous Catalysis. Edited by Robert H. Crabtree

ISBN: 978-3-527-32497-2

Hicham Idriss
University of Aberdeen
Department of Chemistry
Meston Walk
Aberdeen, AB24 3EU
UK

Heiko Jacobsen
KemKom
1215 Ursulines Avenue
New Orleans, LA 70116
USA

Mazaahir Kidwai
University of Delhi
Department of Chemistry
Green Chemistry Research Laboratory
Delhi 110007
India

Ivan Kozhevnikov
Department of Chemistry
University of Liverpool
Liverpool L69 7ZD
UK

Adam F. Lee
University of York
Department of Chemistry
Surface Chemistry and Catalysis Group
Heslington
York YO10 5DD
UK

Nathan S. Lewis
California Institute of Technology
Division of Chemistry and Chemical Engineering
Beckman Institute and Kavli Nanoscience Institute
210 Noyes Laboratory, 127–72
Pasadena, CA 91125
USA

Masaya Matsuoka
Osaka Prefecture University
Graduate School of Engineering
Department of Applied Chemistry
Gakuen-chi, 1-1
Sakai
Osaka 599-8531
Japan

Morgan S. Scott
University of Auckland
Department of Chemistry
Private Bag 92019
Auckland
New Zealand

Frédéric Vogel
Paul Scherrer Institut
Laboratory for Energy and Materials Cycles
5232 Villigen PSI
Switzerland

Anthony Volpe Jr
Symyx Technologies Inc.
3100 Central Expressway
Santa Clara, CA 95051
USA

Don Walker
California Institute of Technology
Division of Chemistry and Chemical Engineering
Beckman Institute and Kavli Nanoscience Institute
210 Noyes Laboratory, 127–72
Pasadena, CA 91125
USA

Karen Wilson
University of York
Department of Chemistry
Surface Chemistry and Catalysis Group
Heslington
York YO10 5DD
UK

1
Zeolites in Catalysis

Stephen H. Brown

1.1
Introduction

Acid catalysis as a modern science is less than 150 years old. From its inception, acid catalysis has been explored as a means of producing fuels, lubes and petrochemicals. Ordinary homogeneous acids, both inorganic and organic, never proved industrially useful at temperatures much above 150 °C. The first reports of aluminosilicate solid acid catalysts involved the use of clays after the turn of the century. The inspiration for the first commercial synthetic aluminosilicate catalysts came from work done co precipitating silicon and aluminum salts during WWI by a Sun Oil chemist [1]. The Brønsted acid site in these materials is most often represented as in Scheme 1.1. Useful features of this novel type of acid versus homogeneous liquid acids were their high temperature stability, moderate acidity (roughly equivalent to a 50% sulfuric acid solution), solid and non-corrosive character and regenerability by air oxidation. These features enabled acid catalyzed reactions of chemicals to be contemplated at a greatly extended range of temperatures (up to 600 °C) and metallurgies.

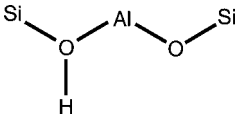

Scheme 1.1 The Brønsted acid site of an aluminosilicate.

The first embodiments of many modern refining processes including heavy oil cracking, naphtha reforming and light gas oligomerization did not use catalysts [2]. As soon as these thermal processes commercialized, exploration of the use of solid acid catalysts ensued naturally.

Because of the key role played in the development of the automotive industry, heavy oil cracking to gasoline provided a focal point for the early development of heterogeneous acid catalysis. Temperatures above 400 °C and pressures below 3 atmospheres are thermodynamically favorable for the conversion of heavy oils to light hydrocarbons rich in olefins. Acceptable heavy oil cracking rates are achieved without a

Handbook of Green Chemistry, Volume 2: Heterogeneous Catalysis. Edited by Robert H. Crabtree

ISBN: 978-3-527-32497-2

catalyst at temperatures above 600 °C. This was the basis of the thermal cracking process. Thermal cracking produces high yields of methane and aromatic hydrocarbons. The goal of researchers was to find a catalyst that could crack heavy hydrocarbons selectively to gasoline with only minimal formation of gases with molecular weights of less than 30. Due to thermodynamic constraints, the catalyst had to be effective at a temperature above 400 °C. In order to avoid unselective thermal cracking, the catalyst had to be effective below 550 °C.

The discovery in the early 1920s by Houdry that acid activated clays were active and selective in this temperature window was a breakthrough [2]. In the 1930s and 1940s methods were developed and commercialized to produce high surface area man-made aluminosilicates that were significantly improved catalysts. Examination of the aluminosilicate catalysts led to the understanding that the active site was a Brønsted acid [3].

At the time of the discovery of synthetic zeolites in the early 1950s, only two classes of solid Brønsted acids (solid phosphoric acid and aluminosilicates) were being used commercially to produce commodity fuels or petrochemicals [4]. The commercialization of silica-rich synthetic zeolites in their hydrogen form represented a breakthrough for scientists and organizations interested in the production of fuels, lubes and petrochemicals at temperatures above 200 °C. Like amorphous aluminosilicates, zeolite Brønsted acid sites are active and stable up to 600 °C. Shortly after Union Carbide's discovery of synthetic zeolites in the late 1940s, Mobil Oil researchers in catalytic cracking of heavy oil investigated zeolites as potential catalysts [5]. The zeolite known as faujasite (FAU) was found to be three to five orders of magnitude more active than amorphous aluminosilicates. Unmodified, FAU was too active to be useful. When the activity of FAU was tuned by ion exchange with rare earth cations and/or by reducing aluminum content, it was found to have a dramatically different selectivity to cracked products. Optimized samples of FAU zeolites produced almost 5% less C_2-gases and coke and increased gasoline yields by more than 10 wt%. Over the course of the past 50 years, evolving heavy oil cracking catalysts and hardware have been continuously decreasing coke and C_2-gas yields while increasing the yield of gasoline.

The commercialization of zeolite catalysts for heavy oil cracking unleashed the creative abilities of every organization interested in producing fuels and petrochemicals using acid catalysts between 250 and 600 °C. Close to 23 processes have been commercialized (Table 1.1). About two-thirds of the processes had no real precedence using homogeneous acids. The other third involved displacement of homogeneous and amorphous acid catalysts. Introduction of zeolite catalysts for the production of commodities has proceeded at a steady pace. Each commercialization has provided an opportunity for zeolite scientists to find improved catalysts.

1.1.1 The Environmental Benefits of Zeolite-enabled Processes

The petroleum industry has been subject to environmental drivers for many decades [6]. Innovations in technology, some driven by more restrictive regulations,

Table 1.1 List of zeolite processes.

Process	Reactor type	Temperature range, °C
Toluene + C9 + aromatics	Fixed	350–450
MSTDP	Fixed	350–450
Cumene via transalkylation	Fixed	150–200
Ethylbenzene via transalkylation	Fixed	230–260
Ethylbenzene	Fixed	180–250
Cumene	Fixed	100–150
Fluid catalytic cracking (FCC)	Fluid	500–550
ZSM-5 in FCC	Fluid	500–550
Gasoil hydrocracking	Fixed	350–475
Distillate hydrocracking	Fixed	280–350
Distillate dewaxing	Fixed	350–450
Wax hydrocracking	Fixed	290–370
Wax hydroisomerization	Fixed	300–350
Gasoline octane enhancement	Fixed	350–450
Reformate upgrading	Fixed	450–550
Light paraffin isomerization	Fixed	240–300
Butene isomerization	Fixed	350–450
Xylene isomerization	Fixed	400–470
Light paraffin aromatization	Moving	450–550
Methanol to gasoline	Fixed	300–400
Methanol to olefins	Fluid	400–500
Aromatics feed treating	Fixed	150–250
Caprolactam	Fluid	350–450

have continuously increased the efficiency of refining processes. The trend is to produce fuels having lower concentrations of heteroatoms and polynuclear aromatics (often referred to as clean fuels) that can be burned to carbon dioxide and water with increasingly lower emissions of NO_x, SO_x and particulate byproducts.

For decades, nearly the entire hydrocarbon content of a barrel of oil feeding a refinery or petrochemical complex has been converted to salable products or used for fuel at the manufacturing site. Distillation of crude oil largely splits it into streams with the boiling ranges of the fuels sold to consumers and businesses (gasoline, diesel, fuel oil, etc.). The quantities of the streams produced by distillation rarely match market demand. Processes using zeolite catalysts have reduced the effort required to convert streams that are oversupplied by simple crude oil distillation into undersupplied products. Optimized zeolite catalyzed processes are often high technology operations. Performance can be sensitive to the performance of neighboring units. Operating multiple zeolite-catalyzed processes can provide refiners with an incentive to continuously work to bring the refinery closer to steady state operation. Adoption of these high technology processes and work practices has helped refiners to steadily increase the amount of clean fuel products produced from each barrel of oil, thereby reducing emissions of CO_2, NO_x, SO_x and particulates and increasing energy efficiency.

Zeolite catalysts are remarkably efficient. Each weight unit of zeolite produces between 3000 and 500 000 weight units of fuel or petrochemical product before its lifetime ends and it is removed from catalyst service. As a result, relatively small volumes of spent zeolite catalysts are produced. There are often other uses for spent catalysts, such as an ingredient for cement. In the many cases where reuse is an option, there are little/no catalyst waste disposal costs.

Catalytic cracking (also known as fluid catalytic cracking or FCC) is by far the most economically important process in the refining and petrochemicals industry and will be described in some detail to allow the green aspects to be highlighted. World wide, FCC units process almost 20 million bbl/day of feedstock (almost 30% of the crude oil produced) and FCC catalysts generate $1 billion in sales [7]. The remarkable performance of the FCC process is achieved by both optimizing the zeolite catalyst and the reactor design. A schematic of an FCC unit is provided in Figure 1.1.

The FCC catalyst spends most of its time in a large, cylindrical regeneration vessel typically 15 meters in diameter and 40 meters tall holding 300 tons of a coarse powder catalyst comprised of a bell-shaped distribution of spheres between 15 and 120 microns in diameter. The vessel is typically held at 15–25 psig and 620 to 700 °C. Air is continuously blown up from the bottom of the vessel and is carefully distributed to provide uniform contacting with the solids. When properly engineered, up flowing gases mix with the coarse catalyst powder to form a mixture which behaves like a fluid. The reaction carried out in the regeneration vessel is the combustion of the solid carbonaceous reaction byproducts that accumulate on the catalyst during the cracking reaction. The FCC catalyst enters the isothermal, back-mixed regenerator at the reaction temperature (about 550 °C) and is heated to the regenerator temperature by the heat of combustion of the coke.

Because of its fluid-like properties in the presence of a flowing gas stream, the catalyst will flow smoothly out of the bottom of the regenerator, up a 2 meter diameter

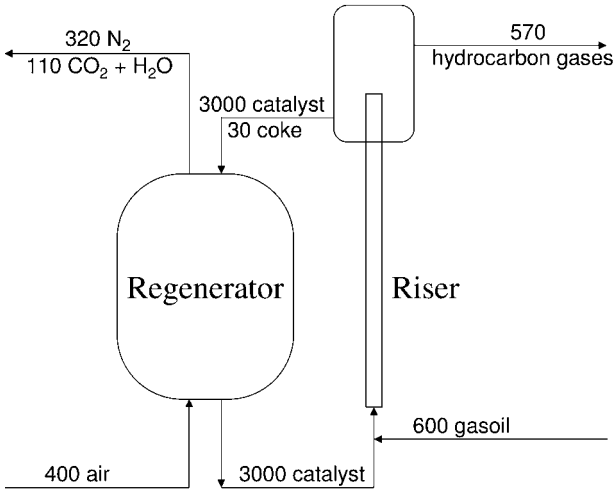

Figure 1.1 FCC reactor process flow diagram.

pipe (called a riser) where it contacts the heavy oil feedstock and then back into the top of the regeneration vessel. A typical catalyst circulation rate for a unit filled with 300 tons of catalyst would be 3000 tons/hour. An average catalyst particle travels through the riser once every 5 or 6 minutes. Heavy oil feedstock is heated to about 300 °C and sprayed into the circulating catalyst (620 to 700 °C) at the bottom of the riser. Feed vaporization is accomplished by direct contact with the hot zeolite catalyst. The gaseous product is removed utilizing cyclones at the top of the riser. Feedstock is typically fed into the riser at twice the total catalyst inventory and one fifth the catalyst circulation rate (e.g. catalyst circulation of 3000 tons/h and a feed throughput of 600 tons/h). The total time of feedstock and catalyst contact is several seconds. About 5 wt% of the feedstock (no more, no less) must be converted to the carbonaceous solids (coke) that are required to provide the energy input needed to drive the feedstock vaporization and the endothermic reaction. A typical catalyst particle contains about 1 wt% coke on catalyst upon entering the regenerator.

Thirty to fifty percent of a barrel of crude oil boils above the endpoint of gasoline and automotive diesel fuels. The FCC unit converts much of this material into gasoline and diesel fuels with roughly 80 wt% selectivity. Another 5 to 10% of the C_4-products are easily converted into high quality gasoline in a second step, resulting in an overall selectivity to gasoline and diesel fuels of 85 to 90%. Five wt% of the feed is converted to coke which is used to supply most of the fuel for the unit (regeneration and separations). The remaining ca. 5–10% of the byproducts are mostly low molecular weight gases (<35) and propane.

Catalyst, oil feedstock and air are the only significant inputs to the process. The removal rate of spent catalyst is roughly 2 wt% per day (6 tons/day from a 300 ton inventory). The catalyst is often used as an ingredient in cement manufacture. If necessary, the gases produced in the FCC regenerator are treated to meet emissions specifications for NO_x, SO_x and particulates.

1.2 General Process Considerations

As illustrated by the FCC example, zeolites are important green technologies that are used in processes conducted on a large scale. Zeolite processes with products produced in quantities of <50 000 000 kg/year make a negligible contribution to the overall environmental credits achieved by zeolites. Zeolite processes carried out on a large scale are listed in Table 1.1. Most of these processes produce plastics, lubricants or fuels. The significant production volumes required place many practical constraints on production methods. Commodity materials almost without exception are produced from commodity raw materials (usually fossil fuels) in one to four catalytic steps. Each step takes place in reactors of a size which can be conveniently fabricated, transported and erected and the reactor must be able to run continuously or semi-continuously for >1 year without shut-down. Three reactor types are employed: fixed bed, fluid bed and moving bed. Commodity processes typically produce between 0.5 and 5 product volumes per reactor volume per hour.

1.3 Zeolite Fundamentals

Basic information about the structures and compositions of known zeolites is readily obtained by consulting the International Zeolite Association (IZA) structure atlas [8] (available on the Internet) or the Handbook of Molecular Sieves [9].

Almost all of the zeolite catalysts used in the processes listed in Table 1.1 share a number of basic features. They are silica rich (Si : Al > 5 and <50). They are manufactured (capable of being synthesized in the lab) and they contain 10 or 12 membered ring channel systems. Up-to-date information about zeolite structures is available from the IZA online structure atlas [10]. At the time of writing, the atlas contained a total of 180 known structure types each assigned a unique three letter code. Since an infinite number of zeolite structures are possible, currently available samples are a negligible fraction of total possible structures. 15 of these 180 structure types are readily synthesized in the laboratory with Si : Al > 5 and <50 and with a 10 or 12 membered ring channel system (Table 1.2). FAU, EMT, FER, LTL and MOR were synthesized first at Union Carbide. MEL, MFI, MFS, TON, MTT, MTW, BEA and MWW were first synthesized at Mobil.

Many more man-made zeolite frameworks are in the IZA database containing 10 and/or 12 membered ring systems. These materials are not included in Table 1.2 because the type materials are pure silica. Examples include CFI, CON, DON, IFR, ISV, SFE, SFF, STF, STT and VET.

Most molecules with less than 7 carbons have critical diameters less than the 5.5 angstrom diameter typical of a 10-ring zeolite pore and can freely diffuse. Many larger molecules also have critical diameters less than 5.5 angstroms. Even molecules the size of 1,3,5 tri-isopropyl benzene can diffuse into 12-ring zeolites

Table 1.2 IZA 10 and/or 12 ring zeolite structures with Si:Al between 5 and 50.

Structure code	Ring size	Diffusional potential
EUO (ZSM-50)	10	1D
MTT (ZSM-23)	10	1D
TON (ZSM-22)	10	1D
NES	10 by 10	2D
FER (ZSM-35)	10 by 8	2D
MFS (ZSM-57)	10 by 8	2D
MWW (MCM-22)	10 by 10	2D
MEL (ZSM-11)	10 by 10	3D
MFI (ZSM-5)	10 by 10	3D
MTW (ZSM-12)	12	1D
LTL	12	1D
MOR	12 by 8	2D
BEA	12 by 12 by 12	3D
EMT	12 by 12 by 12	3D
FAU	12 by 12 by 12	3D

with pore diameters exceeding 7 angstroms. This means that the vast majority of molecules present in distilled petroleum fractions can diffuse in and out of zeolites containing 12-membered rings. Larger ring structures, such as 18-ring VPI-5, have a pore diameter of 12 angstroms. These pores are so big that many small molecules fit in side-by-side and ordinary molecules can not be discriminated by molecular size. Once pore sizes have reached >12–20 angstroms, acid sites inside the pores can be conceptualized in the same fashion as acid sites on amorphous aluminosilicates or on zeolite surfaces. Pores so large place few steric constraints on the polymerization of large molecules into larger deactivating oligomeric structures.

Structures of the zeolite frameworks listed in Table 1.2 are provided at the IZA website. Although all the structures contain 10 or 12 ring pores, each structure has many unique aspects. Each ring system has its own unique size and shape. Some zeolites, e.g. FAU, have large internal cavities, while others contain only one dimensional cylindrical pores (e.g. LTL). Because there are only a handful of unique structures, it should not be surprising that there is often a large difference in performance when these structures are applied.

1.3.1 Other Properties

At temperatures >200 °C zeolite Brønsted acid protons delocalize [11]. At temperatures >550 °C dehydroxylation is initiated and Brønsted acid activity is lost [12]. The presence of steam can retard dehydroxylation. Activity loss by dehydroxylation is commonly reversible as the dehydroxylated zeolite can rehydrate at low temperature and resume its original structure.

Zeolites exchanged with polyvalent metal ions (typically nitrate salts) become acidic upon thermal dehydration and nitrate decomposition [13–16]. Weak Brønsted acid sites can form by hydroxylation of the metal cation. The mechanism is believed to proceed by association of the cation with a specific framework aluminum accompanied by dissociation of water to form a hydroxyl group attached to the cation (Scheme 1.2). For this reason, the addition of polyvalent cations to zeolites directly impacts the number of Brønsted acid sites and total zeolite pore volume but has only a minor impact on the strength of the remaining Brønsted acid sites. Furthermore, zeolites containing polyvalent cations are considerably more complex because both the metal cations and the protons are mobile and because many metal ions are more active for redox reactions than silicon and aluminum. At reaction temperatures between 250 and 500 °C these features generally lead to increased rates of hydrogen transfer reactions and more rapid deactivation explaining the limited use of zeolites exchanged with polyvalent cations.

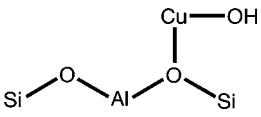

Scheme 1.2 Example of a weak Brønsted acid site in a metal-exchanged zeolite.

1.3.2
Number of Acid Sites

Loewenstein's rule forbids the formation of Al−O−Al bonds in zeolite structures [17]. Therefore, the potential number of acid sites equals the number of aluminum atoms in any reference unit of a zeolite crystal. High silica zeolites (Si : Al > 20) can generally be synthesized and converted to the hydrogen form with minimal deviation from the idealized structure. For these materials the number of acid sites determined by analytical techniques agrees well with the number of acid sites derived from a simple analysis of bulk aluminum content.

1.3.3
Acid Strength

All of the catalysts used in the reviewed processes are aluminosilicates. The overall acid strength of a hydrogen form aluminosilicate zeolite depends upon aluminum distribution. Acidity associated with an aluminum tetrahedra is stronger with a smaller number of near aluminum atoms [18–20]. For this reason, zeolites with Si:Al ratios between 1 and 10 can have a variety of acid site strengths. However, careful studies with ZSM-5 demonstrated that acid sites with 0 and 1 next nearest neighbor aluminums are very close in acid site strength [21]. Most of the acid sites in zeolites with Si : Al ratios >10 have only a small number of their sites with more than one aluminum next nearest neighbors leading to uniform acid site strength. The strength of this site has been well characterized by NMR and IR probes of simple sorbates allowing the conclusion to be reached that the acid site strength is similar to that of 70% sulfuric acid [22–24]. Careful studies of model compound reactions uncomplicated by mass transfer limitations or fast secondary reaction provide further support for uniform acid site strength [25–27].

At the present time, aluminosilicate zeolites remain the only class of crystalline solid Brønsted acids to find broad use in the production of commodity chemicals. Although a wide range of materials with alternative framework compositions are known, few commercial uses have been found for these materials.

Zeolite frameworks and novel frameworks based on aluminophosphate building blocks were discovered at Union Carbide in the early 1980s [28–30]. When phosphorus sites are substituted with silicon, a Brønsted acid is formed. The acid site in these materials is weaker than an aluminosilicate acid site.

1.4
Reaction Mechanisms

1.4.1
Hydrocarbon Cracking

Academic work in the 1930's and 40's elucidated how $AlCl_3$ – a strong Lewis acid – is converted when dissolved in hydrocarbon fractions to a working catalytic species with

strong Brønsted acidity (Scheme 1.3) [31–33]. The basic mechanistic features of hydrocarbon cracking were well understood by the end of the 1950's and are well explained in many subsequent reviews [34–39]. Any unsaturated molecules (i.e. aromatics, olefins, dienes) in hydrocarbon streams undergo protonation in the presence of a Brønsted acid catalyst. Once protonated, isomerization reactions can proceed. In general, hydride shifts proceed considerably faster than alkyl shifts (Scheme 1.4). Exact relative rates are dependent upon the structure of the hydrocarbon, the catalyst and the conditions and need to be computed or measured on a case by case basis.

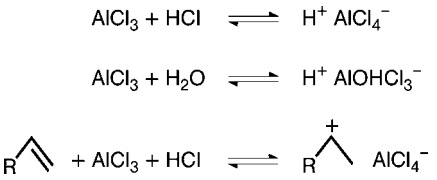

Scheme 1.3 Example $AlCl_3$ activation reactions.

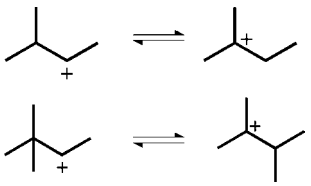

Scheme 1.4 Hydride and methyl shifts.

Once protonated, a hydrocarbon molecule is destabilized, existing almost simultaneously as many different carbocations. The energy of most hydrocarbon carbocations are now well understood and can be calculated using algorithms derived from first principles [40]. In most cases it is safe to assume that a representative sample of a specific protonated hydrocarbon exists at any instant with the full pool of its possible cation isomers populated at a distribution at least approaching thermodynamic equilibrium. Because carbocations are stabilized by delocalization and electron donating groups, isomers containing these attributes dominate the instantaneous distribution (Scheme 1.5, for example). The most stable cations, however, can be less reactive and therefore may not be the most important intermediates of the reaction pathway.

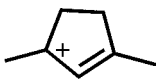

Scheme 1.5 Sample of a cation stabilized by conjugation and branching.

Acid cracking of cations proceeds most readily via beta scission. Aromatics dealkylation is the least complex as it is dominated by a single class of beta scission reaction (Scheme 1.6). There are many viable cracking pathways for paraffin, olefin and naphthene-derived hydrocarbon cations. Cracking of these species is dominated

by beta scission pathways A, B1, B2 and C (Scheme 1.7) [41]. Relative rates of these reactions along with cracking reactions involving primary cations (pathways D and E, Scheme 1.7) have been determined using model compounds and ZSM-5 catalysts at cracking conditions typical of the industrial processes covered in this review (Tables 1.3 and 1.4) [42]. The combined data from the tables demonstrate that large, branched olefins are readily cracked. Through successive cracking and oligomerization reactions, zeolite catalysts can convert such molecules to a broad distribution of olefins directed by thermodynamic considerations at temperatures below 200 °C.

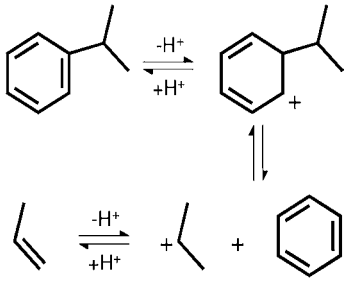

Scheme 1.6 Aromatics cracking reaction.

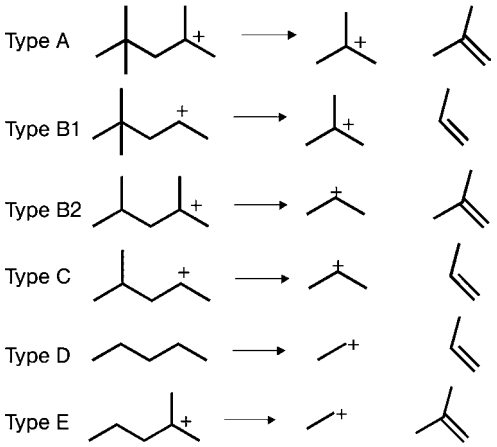

Scheme 1.7 Hydrocarbon cation cracking types.

Table 1.3 Cracking rate constants of hydrocarbons over HZSM-5 at 510 °C.

Carbon #	Rate constant k sec^{-1} olefin	Rate constant k sec^{-1} paraffin
4		0.1
5	10	0.3
6	230	0.8
7	1800	1.5
8	5700	2.2